 DOI: 10.1002/masy.200651022

Characterization of PVA and Chitosan/PVA Blends Prepared from Aqueous Solutions of Various Na_2SO_4 Concentrations

Petronela Drambei,[1] *Yumiko Nakano,*[1] *Yuezhen Bin,*[1] *Tsumuko Okuno,*[2] *Masaru Matsuo**[1]

Summary: Uniplaner orientation of a particular crystal plane along the surface of a film was investigated for poly (vinyl alcohol) (PVA) film prepared by a coagulation bath with concentrated aqueous solution containing 100 ~ 300g of Na_2SO_4 against 1 ℓ of water. The orientation distribution functions of the three crystallographic principal axes of the dried films were obtained by the X-ray diffraction technique. The same treatment was carried out for the films prepared by stretching biaxially of the fresh gel and then by drying the resultant fresh gel. The very high preferential orientation of the crystal chain axes and amorphous chain segments could be realized by the biaxially elongation. Accordingly, the techniques were applied to the biaxially stretching of chitosan and PVA blend films with high Young's modulus. The planer orientation of the chain axes of chitosan and PVA crystallites could be confirmed. The morphology of the film surface was estimated by measurements of contact angle and electron spectroscopy for chemical analysis. The results suggested that the admixture of chitosan decreases wet ability of the specimen and this tendency was slightly enhanced by the biaxially elongation.

Keywords: biaxially stretching; chitosan/PVA blends; films; X-ray; Young's modulus

Introduction

The uniplaner orientation of a particular crystal plane along the surface of a film has been reported for some crystalline polymers under biaxial stretching. This characteristic orientation has been mostly found for the crystal plane having the highest electron density within the unit cell. For example, the each preferential plane for polyethylene (PE)[1] and poly (vinyl alcohol) (PVA)[2] films corresponds to the (110) plane, when the c-axis is chosen as the crystal chain axis. The orientation behavior under the stretching was estimated in terms of the orientation distribution function of the crystallites. The uniplaner orientation of the particular orientation of the (hk0) plane causes the orientation of the chain axes parallel to the film surface automatically and Young's modulus increases with increasing the planer orientation degree of the chain axes. On the other hand, the wet spinning method is well-known to prepare polymer fibers with no melting point, which has been adopted for preparing fibers of PVA, cellulose and poly (acrylonitrile)-(PAN).

It is well-known that the PVA films can be prepared by a coagulation method as has been reported for regenerated cellulose from viscose solution[3] by the coagulation bath with concentrated aqueous solution containing Na_2SO_4. In the method, the (110) plane of PVA crystal has been found to be oriented parallel to the film surface. The method is slightly classical, since the PVA film can be obtained by the gelation/

[1] Department of Textile and Apparel Science, Nara Women's University, Nara 630-8263, Japan
[2] Faculty of Human Environmental Sciences, Mukogawa Women's University, Nishinomiya 663-8558, Japan
E-mail: matsuo@cc.nara-wu.ac.jp

crystallization method from dimethyl sulfoxide and water mixed solvent[1,3–5]. However, the chitosan does not dissolve in the mixed solvent and then the gelation/crystallization method cannot be adopted to prepare blend films of PVA and chitosan.

This paper deals with two purposes by using coagulation method. One is an estimation of the preferential orientation of PVA chain axes parallel to the film prepared by coagulation. This information is important to obtain the films whose orientation of crystallites is random around the film normal direction. The simultaneous biaxially stretching of the PVA fresh gels was also carried out to improve drastically the preferential orientation degree of the c-axes and to obtain high modulus films with isotropic mechanical property around a film normal direction. The second is the preparation of PVA films containing chitosan to develop recyclable films with high modulus from the viewpoints of environmental protection and ecology. In doing so, simultaneous biaxial stretching was carried out by using the blend gels of chitosan and PVA.

Experimental Section

Sample Preparation

Test specimens of PVA, the degree of polymerization being 2000 and the degree of saponification being 99–100 mol%, were prepared into film shape from concentrated aqueous solution of 100 ~ 300g of Na_2SO_4/ℓ concentration by pouring into a glass plate and dipping the plate into various coagulation baths of different compositions as listed in Table 1.

The fresh gel films thus obtained were leached in running water for ca. 1h and dried in ambient condition either with the dimensions fixed by clamping the film between two metallic flanges. The dimensional changes of each specimen at various stages of film formation and the moisture content of each fresh gel film with respect to air dry state are listed in Table 2.

Table 1.
Composition of the coagulation bath.

Bath code	
A bath	Na_2SO_4 100g/l
B bath	Na_2SO_4 200 g/l
C bath	Na_2SO_4 300 g/l

The capital letter in the specimen code corresponds to the specification code of coagulation bath in Table 1 and the subscript 1 and 2 indicate drying of the fresh gel films performed under the conditions of free and fixed dimensions, respectively. The fresh gel prepared from C-bath was stretched biaxially. The detailed method is described later.

As can be seen in Tables 1 and 2, the higher the Na_2SO_4 concentration in the coagulation bath, the more anisotropic shrinkage of the specimen, i.e., the stronger the dehydrogenated power of the bath, the greater is the shrinkage in the thickness direction compared with that along the surface at every stage of the film formation, and the less the water content of the gel film.

The preparation of chitosan and PVA composite films was done by using the coagulation method discussed for the PVA films above. According to the established methods[6–11], chitosan/PVA blend films were prepared from 4% concentration of chitosan, dissolved in 2% acetic acid and 6% PVA, dissolved in water at 90–95°C for 40–50 min, under nitrogen gas. Chitosan with 85% degree of deacetylation and PVA were used as test specimens. Solution of chitosan (4%) and acetic acid (2%) was stirring about 5 ~ 6 hours at room temperature.

PVA aqueous solution (6%) was prepared by stirring at 95°C for 40–50 minutes and cooled down to room temperature. Chitosan and PVA solutions, the composition of chitosan/PVA being the 25/75, were mixed and stirred at room temperature for ca. 2 weeks without cover, to promote evaporation of water. After evaporating water, the concentration of the blend solution became higher and reached about 30%. The viscous blend solution was spread on a glass and immersed for 24 hours

Table 2.
Specimen contraction during coagulation and drying and water content of fresh gel film.

Specimen code[a]	Degree of surface shrinkage (%)[b]		Degree of thickness shrinkage (%)		Water content of fresh gel (%)[c]
	(V-G)/V	(V-D)/V	(V-G)/V	(V-D)/V	
A_1	0.161	0.489	0.465	0.569	482
B_1	0.161	0.466	0.581	0.662	467
B_2	0.152	0.152	0.581	0.790	467
C_1	0.146	0.453	0.694	0.814	422
C_2	0.146	0.146	0.694	0.885	422
D_1	0.115	0.416	0.514	0.810	422

[a] Capital letters in the specimen codes correspond to the bath code in Table 1 and the subscripts 1 and 2 correspond, respectively, to drying with the film unconstrained and with fixed dimensions.
[b] The letters V, G and D denote viscose solution, gel and dried film.
[c] The water content of fresh gel is defined with respect to the air-dried film.

in Na_2SO_4 solution (30% concentration). The sample was washed in plate water and air dried. The preparation of chitosan/PVA blend films was also accomplished by the method similar to the preparation of PVA films.

The PVA gel and chitosan/PVA composite gel were cut into squares of 90×90 mm. The samples were immersed in water and kept for 30 min, to absorb water molecules, which play an important role as plasticizer under elongation. The simultaneous biaxially stretching of the films were carried out by an Iwamoto biaxial stretcher, at room temperature. After the stretching, the films were fixed on the stretching machine for 3 days in order to assuring high dimensional stability. The dimensional changes of the specimen are listed with code D_1 in Table 2.

Experimental Procedure

Sample Characterization

Contact angle was determined by the shape of a liquid droplet on the film surface by using a Kyowa Kaimen Science Instrument CA-X[12].

The surface was analyzed by electron spectroscopy for chemical analysis by using Shimazu, ESCA-850. The sample was irradiated with monochromated M_gK_α X- rays (8kV, 30mA) and the scanning speed is 0.05V/s to find the atoms of surface.

The complex dynamic tensile moduli were measured at a frequency of 10 Hz over the temperature range from -150 to 250°C by using a viscoelastic spectrometer (VES-R) of Iwamoto Machine Co. Ltd. The detailed method was described elsewhere[13].

Orientation Distribution of PVA Chains Within the Film

The X-ray measurements were carried out with a 12 kW rotating-anode X-ray generator (Rigaku RDA-rA) operated at 150 mA and 40 kV. When crystallites within the film are oriented randomly around the film thickness direction, the best way is to direct an incident X-ray beam parallel to the film surface. Of course, the diffraction peak was detected at $2\theta_B$, the angle between an incident beam and the film normal direction was tilted at θ_B. However, the diameter of irradiated X-ray beam is much larger than cross section area of the film thickness. Accordingly, we developed a small but refined instrument to stack a number of thin films as shown in Figure 1[2].

In such a stacked condition, measurements of the X-ray diffraction intensity could be performed using a horizontal scanning type goniometer, operating at a fixed time step scan of 0.1/40 s over a range of twice Bragg angle $2\theta_B$ from 15 to 40°. This method is much better than pole-figure method to obtain the high diffraction intensity. The intensity distribution was measured as a function of a given rotational angle θ_j by rotating about the stretching direction at $2 \sim 5^\circ$ interval from 0 to 90°. θ_j is

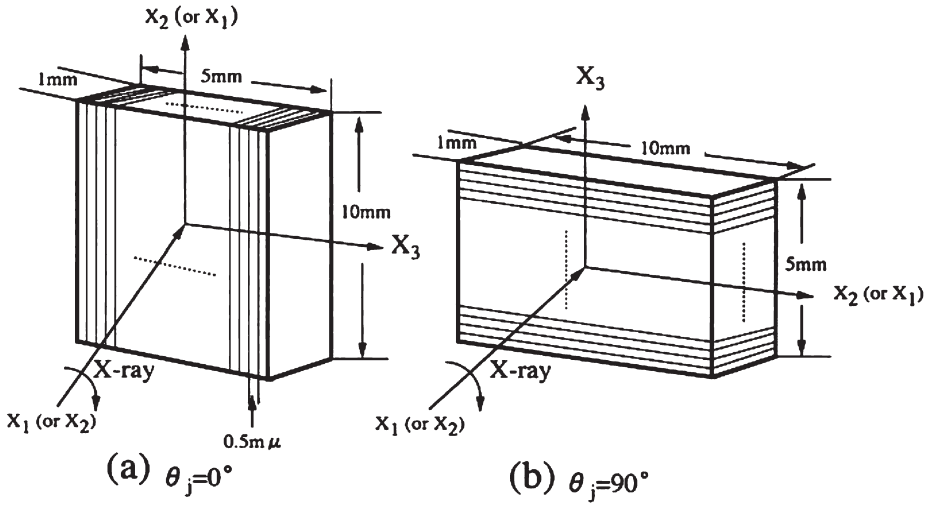

Figure 1.
Thin stacked films for measuring X-ray diffraction intensity distribution as a function of twice the Bragg angle at (a) $\theta_j = 0^\circ$ and (b) $\theta_j = 90^\circ$.

0° and 90° in Figure 1a and 1b, respectively. According to the crystal structure of poly (vinyl alcohol) proposed by Nitta et al.[14], the diffraction intensity distribution at twice the Bragg angles, 19.3, 20.0 and 22.8° for the (110),(1$\bar{1}$0)and (200) planes, respectively, may be available for evaluating the crystal orientation. After applying corrections to the observed X-ray diffraction intensity, such as air-scattering, background noise, polarization, absorption, and incoherent scattering, and subtracting the contribution from the amorphous scattering from the corrected total intensity by using a method similar to that proposed by Sakurada et al.[15], the crystal diffraction intensity distribution was separated into respective contributions from the (110),(1$\bar{1}$0)and (200) planes. In this procedure, it may be expected that each contribution has a symmetric distribution given by Lorenz function of twice the Bragg angles[1)].

$$Icry(2\theta_B) = \sum_{j=1}^{3} \frac{I_j^o}{1 + (2\theta_j^o - 2\theta_B)^2 \Big/ \beta_j^2} \qquad (1)$$

Here β_j is the half-width of the j-th peak at half of the peak intensity and θ_j^o is the Bragg angle at which the maximum intensity of the j-th peak appears. In this system, the (110),(1$\bar{1}$0)and (200) planes correspond to $j = 1$, 2 and 3. Using the same process at a given θ_j in the range from 0 to 90°, the intensity distribution $I_j(2\theta_B)$ can be determined for the respective j-th plane after integrating $I_{cry}(2\theta_B)$ by $2\theta_B$ at each θ_j, and consequently the orientation distribution function $2\pi q_j(\cos\theta_j)$of the reciprocal lattice vector of the j-th plane may be given by

$$2\pi q_j(\cos\theta_j) = \frac{I_j(\theta_j)}{\int_0^\pi I_j(\theta_j)\sin\theta_j d\theta_j} \qquad (2)$$

The degree of the second order moment of the j-th reciprocal lattice vector may be given by

$$\left\langle \cos^2\theta_j \right\rangle = \frac{\int_0^\pi I_j(\theta_j)\cos^2\theta_j \sin\theta_j d\theta_j}{\int_0^\pi I_j(\theta_j)\sin\theta_j d\theta_j} \qquad (3)$$

Thus, the second order orientation factor of the j-th reciprocal axis may be given by

$$F_{20}^j = \left\{ \frac{3\left\langle \cos^2\theta_j \right\rangle - 1}{2} \right\} \qquad (4)$$

The second order factor of the three principal axes, F_{20}^a, F_{20}^b and F_{20}^c can be obtained by the measured values of $F_{20}^{[110]}$, $F_{20}^{[1\bar{1}0]}$ and $F_{20}^{[200]}$ by using the relationship given by Roe

and Kribbaum[16]. The degree of orientation of non-crystalline chain segments in terms of the same quantity as that for the b-axis, F_{20}^{am} can be evaluated on the basis of the simple additive role of crystalline and amorphous contributions to the total (bulk) birefringence of the specimen. The second order orientation factor of the amorphous chain segments was obtained from the birefringence as estimated by the subtraction of the crystalline contribution from the total birefringence, assuming simple additivity as indicated in the following equation[17].

$$\Delta_{total} = X_c\Delta_c + (1 - X_c)\Delta_a + \Delta_f \quad (5)$$

where Δ_{total} is the total birefringence of the bulk specimen, Δ_c, the crystalline birefringence, Δ_a the non-crystalline birefringence, X_c the volume fraction of the crystalline phase, and Δ_f the form birefringence. Δ_c and Δ_a are given by

$$\Delta_c = n_aF_{20}^a + n_bF_{20}^b + n_cF_{20}^c = (n_c - n_a)F_{20}^c + (n_b - n_a)F_{20}^b \quad (6)$$

and

$$\Delta_a = (n_{//} - n_\perp)F_{20}^{am} \quad (7)$$

where n_a,n_b and n_c are the refractive indices along a, b and c-axis, which are given as 1.737, 1.717, and 1.827, respectively. $n_{//}$ and $n_\perp$ are the refractive indices parallel and perpendicular to an amorphous chain segment. The intrinsic birefringence of $(n_{//} - n_\perp)$ of the amorphous chain segment is 88×10^{-3} and F_{20}^{am} is the second-order orientation factor of the amorphous chain segments. The procedure for evaluating the intrinsic birefringence of crystalline and amorphous phases is quite similar to that described earlier. These values were estimated by utilizing the values of bond polarizabilities proposed by Clement[18], the crystal structure by Nitta et al.[14] and the values of intrinsic crystal and amorphous densities (1.345 and 1.269, respectively) by Sakurada et al.[13] The orientation factors, F_{20} characterize the molecular orientation distribution with variation between −1/2 and 1. In a simultaneous biaxially stretched film, they are zero for a random orientation, while for complete orientations parallel and perpendicular to the film normal direction, they are 1 and −1/2, respectively. By neglecting Δ_f, the second order orientation factors of the c-axes and the amorphous chain segments may be calculated through Eqs. (5) ~ (7).

Results and Discussion

PVA Films

Tables 3 and 4 show the second order orientation factors of the reciprocal lattice vectors of the (110), $(1\bar{1}0)$and (200) planes of PVA crystals observed and those of the principal crystallographic axes of the crystal unit calculated respectively, with respect to the film normal direction X_1 axis. The same quantity for the orientation of the non-crystalline chain segments is listed in Table 4. The subscript 3 indicates drying of the fresh gel film under a condition of simultaneously biaxially stretching up to extension ratio with 2×2.

From the above results, it may be suggested that the uniplaner orientation of the (110) plane and the planer orientation of the c-axis and non-crystalline chain segments along the film surface became higher with increasing Na_2SO_4 content, and that the above uniplaner and planar orientations are obvious not only for the specimens biaxially stretched but also for the specimens dried with fixed dimensions, rather than with free dimensions, even from the fresh gel coagulated in the bath A having relatively low dehydrating power.

Table 3.
The second order orientation factors of the reciprocal lattice vectors of the (110), $(1\bar{1}0)$and (200) planes of poly (vinyl alcohol) crystals.

Specimen code	$U_{(110)}$	$U_{(1\bar{1}0)}$	$U_{(200)}$
A_1	0.346	0.294	0.325
B_1	0.451	0.247	0.311
B_2	0.490	0.226	0.311
C_1	0.457	0.202	0.318
C_2	0.543	0.180	0.390
A_3	0.692	0.141	0.351

Table 4.
The second order orientation factors of the three principal crystallographic axes.

Specimen code	U_a	U_b	U_c	Non crystalline chain segment
A_1	0.296	0.473	0.202	0.211
B_1	0.278	0.532	0.158	0.149
B_2	0.295	0.540	0.129	0.126
C_1	0.282	0.574	0.109	0.114
C_2	0.350	0.549	0.062	0.092
A_3	0.310	0.615	0.034	0.138

Especially, the degree of the uniplaner orientation of the biaxially stretched film was the highest among all the specimens.

For the coagulation of regenerated cellulose film from viscose solution, similar uniplaner orientation of the (110) plane of cellulose II crystal was observed. The orientation behavior was explained in terms of the slip of crystallites between the hydrated (110) planes. Moreover, the (110) plane within the crystal unit[19] was the highest electron density which is associated with the lower dislocation energy[20]. The (110) plane as the hydrated plane has been supported by comparing the lattice constant of the (110) plane in hydrated state with that in the dry state[3].

The uniplaner orientation of the (110) plane and the planner orientations of the c-axis and of the non-crystalline chain segment, as observed above during coagulation as well as biaxial stretching of the PVA films, may be explained in terms of the slip of the (110) planes associated with its orientation so as to parallel to the planar stress in the system. For a PVA crystal unit, both the (110) and,$(1\bar{1}0)$ planes are assigned as the hydrogen-bonding planes in addition to the fact that the (110) plane has the highest electron density. Hence as reported for regenerated cellulose films[3], the preferential uniplaner orientation of the (110) plane, especially during coagulation, must be attributed to lowering of the dislocation energy of the plane due to the hydration[20].

Here it may be noted that the drastic preferential orientation of the amorphous chain segments could be observed for the film elongated biaxially as shown in Table 4. The orientation degrees are the highest. The gels containing water tended to shrink drastically after removing the stretcher indicating rubber elasticity[1]. Then, it is evident that the preferential orientation of the (110) plane parallel to the film surface is derived by the planner stress derived under the evaporation of solvent, when the gel was dried at the fixed state. Namely, the slippage of the crystallites on the (110) plane was attributed to the planner stress leading to the restriction of the shrinkage of the non-crystalline chain segments. The mechanism of the slippage on the (110) plane is thought to be similar to the plastic deformation of metal crystals assuring the minimum dislocation energy[20]. The uniplaner orientation of the (110) plane causes the preferential orientation of the c-axes parallel to the film surface and this orientation behavior may be expected to provide the improvement of the Young's modulus of the films with isotropic mechanical properties around the film normal direction.

Based on this concept, the preparation of the chitosan and PVA blend films was done by using the above coagulation method for the PVA films.

Chitosan and PVA Blend Film

Figure 2 shows a WAXD pattern detected from the side view of chitosan film. The film was prepared by a casting method without coagulation process only to check the diffraction peaks from chitosan crystallites. Here we must emphasize that the film prepared by casting cannot be elongated biaxially. The pattern shows the diffraction from chitosan crystallites. The arcs at inner side belong to the diffraction from the (100) plane at $2\theta_B = 10.2$, while the arcs at outer

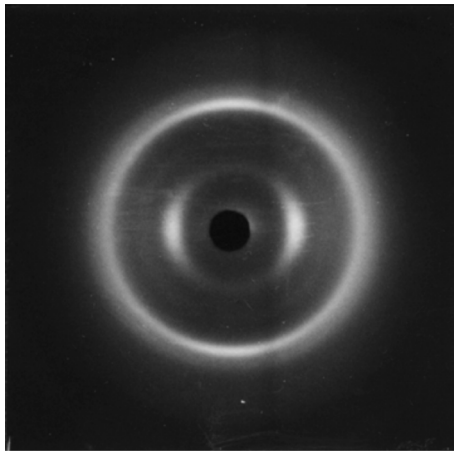

Figure 2.
WAXD pattern for a chitosan film.

side belong to the overlapped diffraction from the (002), (120) and $(10\bar{2})$ planes at $2\theta_B = 19.9 \sim 22.0$.

Figure 3 shows the X-ray diffraction intensity curves from the chitosan (100/0), PVA (0/100) and for the blend films prepared by casting method. The open circle show the overlapped experimental intensity and the rough and fine dotted lines by the peak separation belong to the diffraction intensity distributed from PVA and chitosan crystallites, respectively. The solid curve is the summation of the two separated curves and it is in good agreement with the experimental curves. The curves show the same profile indicating no thermal crystallization. The peaks appeared at 19.3° and 20.2° belong to PVA and chitosan crystallites, respectively and the peak positions were maintained independent of the chitosan/PVA compositions, which indicates that blending gave no effect on the crystallization of the two polymers. Namely, the observed curve represented by open circles shows the simple overlapped peaks from the individual PVA and chitosan crystallites. This means that the crystallization of PVA and chitosan occurred independently under evaporation of solvent.

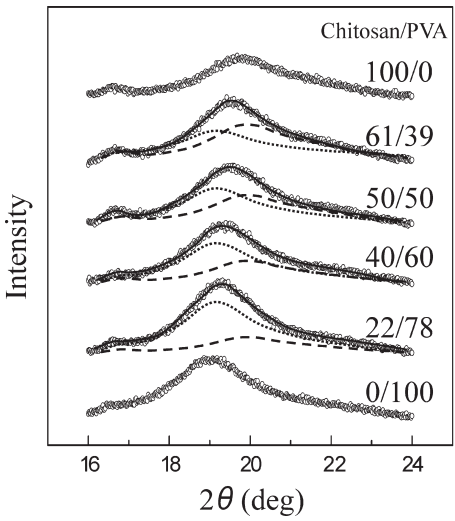

Figure 3.
X-ray diffraction intensity curves of chitosan, PVA and blend films.

Based on the results in Figures 2 and 3, it was found that the diffraction peaks from crystal planes of chitosan and PVA are overlapped indicating that the peak separation of overlapped peaks was impossible, since the PVA peak composes of the diffraction peaks from (110) and $(1\bar{1}0)$. The peak separation for the three peaks is impossible.

Then, the diffraction pattern from the blend film elongated up to 2×2 times is shown in Figure 4, in which an incident X-ray beam was directed parallel to the film surface.

The sample preparation was done in the coagulation bath with aqueous solution containing 300 g/ℓ. It is evident that the admixture of chitosan into PVA hampered the uniplaner orientation of the (110) plane of PVA crystallites because of the drastic decrease of the intensity from the overlapped peak from chitosan and PVA within the blend film, which indicates poor planner orientation of the c-axes of PVA crystallites. This indicates that biaxial stretching is meaningless to promote the Young's modulus. In order to check it, the temperature dependence of the complex dynamic modulus was measured for PVA and chitosan/PVA blend films.

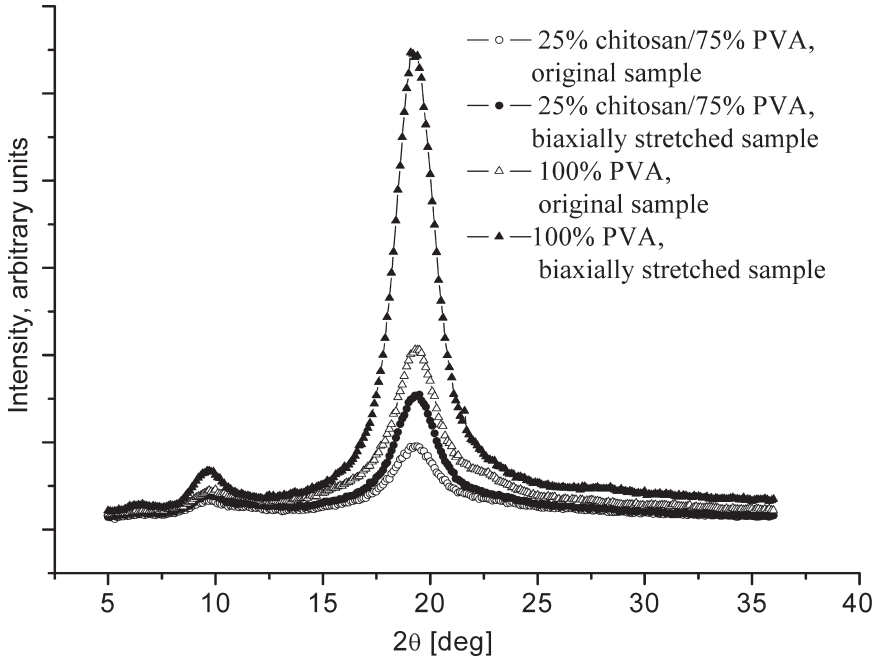

Figure 4.
X-Ray patterns of Chitosan/PVA and PVA - parallel to the surface.

Figure 5(a) and (b) show the storage (E′) and loss (E″) moduli, respectively, as a function of temperature. From Figure 5(a) it is seen that the curves of E′ for all the films decrease significantly with increasing the temperature and tends to level off beyond 20°C. Interestingly, the storage modulus (E′) for the undrawn chitosan/PVA blend films is higher than that of the drawn PVA films. The E′ increased by biaxially stretching but this tendency is very small and the admixture of chitosan provided significant increase in E′, indicating that planer orientation of the chain axes by biaxially stretching up to 2×2 times is not effective to increase Young's modulus. In contrast, the admixture of chitosan plays an important role to increase Young's modulus and to prepare recycling films with high modulus from the viewpoint of environmental protection and ecology.

The value at 20°C for drawn blend film was ca. 6 GPa, which is about the half of the ultimate goal of Young's modulus of an ideal PVA film whose cristalinity is 100% and the second order orientation factor was −1/2 indicating perfect planner orientation of the c-axes[1)].

Figure 5(b) reveals that each of the complicated profiles of loss modulus of PVA and chitosan/PVA blend films contain three peaks indicating three relaxation modes: the local segmental motion at lowest temperature side, the active mobility of the amorphous chain segments by water playing as plasticizer at middle temperature range and thermal mobility of the chain segments at the higher temperature side. This phenomenon was discussed elsewhere in detail[21].

Table 5 shows contact angles measured for the PVA and chitosan/PVA blend films. The contact angles of the blend films are much higher than those of PVA films, indicating that wet-ability of the chitosan/PVA blend films is essentially lower than that of PVA film. The angles of the undrawn and drawn chitosan/PVA films are closer each other, while the angle for PVA films become slightly smaller by the elongation. This means that the wet-ability for PVA films increases by biaxially stretching,

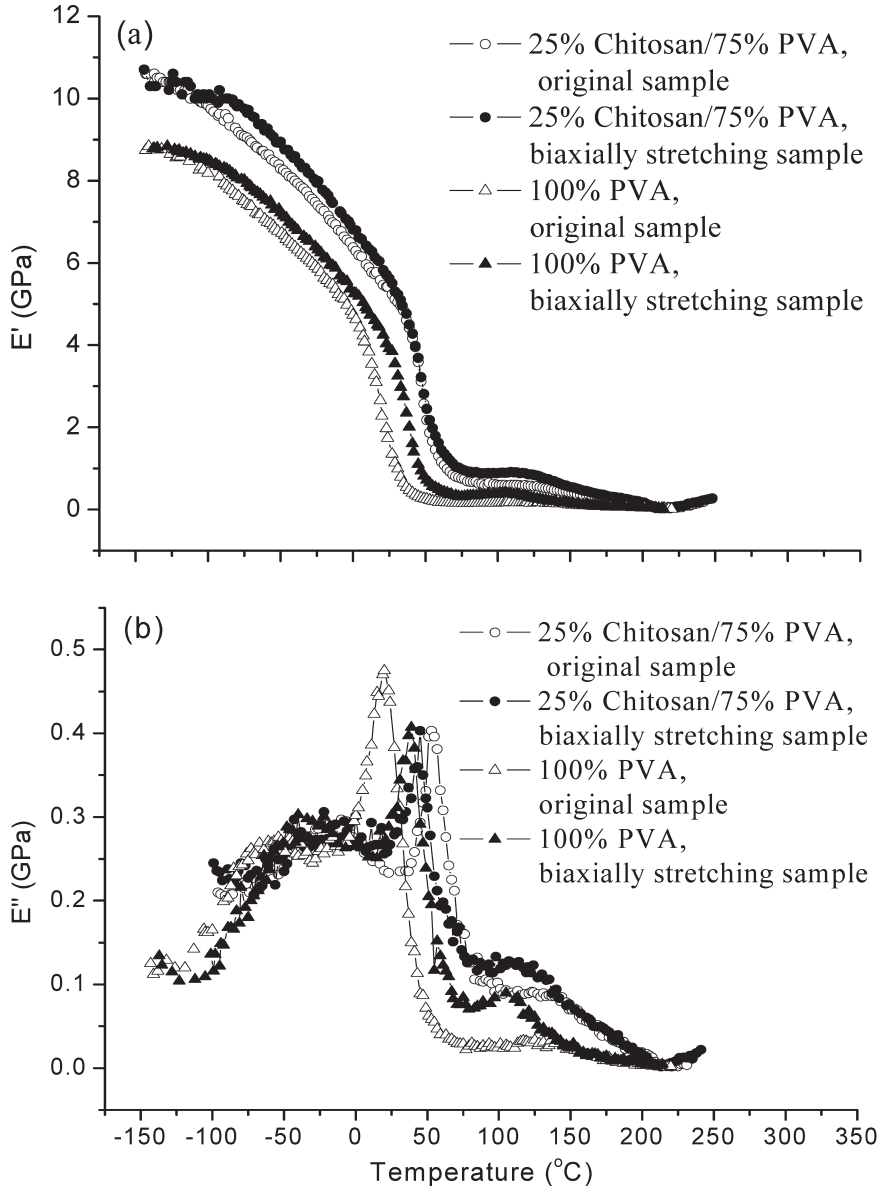

Figure 5.
(a) Storage modulus (E′) and (b) loss modulus (E″) of Chitosan/PVA and PVA films, as a function of temperature.

Table 5.
Contact angles (degree) of chitosan, the blend (25/75) and PVA films.

Sample	Chitosan	25/75 blend		PVA	
	Original	Original	Drawn	Original	Drawn
Average angle	91.9	91.7	91.2	75.3	71.8

while that for chitosan/PVA blend films is independent of the elongation.

The Electron Spectroscopy for Chemical Analysis (ESCA) has been used to evaluate the chemical structure of the 25/75 blend and PVA for the surface of undrawn and drawn films. Table 6 shows the ratio

Table 6.
The values of O/C for PVA films and O/C and N/C for chitosan film and 25/75 blend films.

Sample	N/C	O/C
Undrawn chitosan film	0.1079	1.182
Undrawn blend film	0.0169	0.947
Drawn blend film	0.036	0.963
Undrawn PVA film		0.867
Drawn PVA film		1.656

of nitrogen (N)/carbon (C) and that of oxygen (O)/C, for chitosan/PVA blend films and (O)/C for PVA films. The ratio of O/C for the drawn PVA film is higher than that of the undrawn film, indicating the appearance of OH groups on the film surface leading to the diffusion of PVA chains to the film surface. This satisfies the result that the contact angle for the drawn films became lower than that of the undrawn films.

On the other hand, the data in Table 6 provide that the ratios of O/C and N/C for the drawn blend film are slightly higher than those of undrawn film. The very small increase in the ratio of N/C by the elongation is related to the slight diffusion of chitosan molecular chains to the film surface. The results in Table 5 and 6 suggests that the admixture of chitosan provided an increase in O/C of the undrawn blend film but the wet ability of the corresponding blend film is lower than that of the PVA film.

Through a series of experimental results, the significant effect of the admixture of chitosan was an increase in the storage (Young's) modulus and the decrease in wet ability.

Conclusion

PVA and chitosan-PVA blend gels were prepared in a coagulation bath with concentrated aqueous solution containing Na_2SO_4 and dried at ambient condition. The following concluding could be derived:

1. The preferential orientation of the crystal axes and amorphous chain segments within the PVA films was pronounced as the concentration of Na_2SO_4 increased. The further increase of the orientation was achieved by biaxial elongation of the gel film.
2. The above method could be applied to the blend films of chitosan and PVA. The planner orientation of chitosan and PVA chains could be confirmed but the quantitative analysis was impossible, since the peaks of chitosan and PVA crystallites were overlapped. The storage (Young's) modulus was effective by the admixture of chitosan into PVA rather than biaxial stretching.
3. By the admixture of chitosan into PVA, the wetability of the blend films was confirmed to be lower than that of PVA films. The measurements of ESCA allowed the analysis of the chemical structure of the surface of the films. The ratios of O/C and N/C for the drawn PVA film are higher than that of the undrawn film, indicating the movement of chitosan chains to the film surface.

[1] Y. Bin, Y. Tanabe, C. Nakabayashi, H. Kurosu, M. Matsuo, Polymer **2001**, 42, 1183.
[2] T. Nakashima, C. Y. Xu, Y. Bin, M. Matsuo, Polymer J. **2001**, 33, 54–68.
[3] M. Matsuo, S. Nomura, H. Kawai, J. Polym. Sci., Polym. Phys. **1973**, Ed. 11, 2057.
[4] M. Matsuo, Y. Sugiura, S. Takematsu, T. Ogita, T. Sakabe, R. Nakamura, Polymer **1997**, 38, 5953.
[5] M. Matsuo, Y. Bin, M. Nakano, Polymer **2001**, 42, 4687–4707.
[6] M. Ratajska, M. Wisniewska-Wrona, G. Strobin, H. Struszczyk, S. Boryniec, D. Ciechanska, Fibers and Text in Eastern Europe **2003**, 11, 59–63.
[7] M. Ratajska, G. Strobin, M. Wisniewska-Wrona, D. Ciechanska, H. Struszczyk, S. Boryniec, D. Binias, W. Binias, Fibers and Text in Eastern Europe **2003**, 11, 75–79.
[8] H. Sashiwa, N. Kawasaki, A. Nakayama, E. Muraki, N. Yamamoto, H. Zhu, H. Nagano, Y. Omura, H. Saimoto, Y. Shigemasa, S. Aiba, Biomacromolecules **2002**, 3, 1120–1125.
[9] H. Sashiwa, N. Yamamori, Y. Ichinose, J. Sunamoto, H. Yajima, S. Aiba, Chitin, Kitosan Kenkyu (Chitin chitosan Res.) **2003**, 9, 205–210.
[10] M. H. Struszczyk, Chitin and chitosan - part II. Some aspects of biodegradation and bioactivity, Polymery (Warsaw) **2002**, 47, 619–629.

[11] A.H. Zheng, J.Q. Gao, Y.P. Zhang, W.Q. Liang, Biochem Biophys Res Commun **2004**, 323, 1321–1327.
[12] Tsumuko Okuno, Yumiko Nakano, Kyoko Yoshida, Kotaro Yokoyama, Maki Hamaguchi and Masaru Matsuo, Polymer J. **2005**, 37, (3), 169–176.
[13] M. Matsuo, C. Sawatari, T. Ohhata, Macromolecules **1988**, 21, 1317–1324.
[14] I. Nitta, I. Taguchi, Y. Chatani, Ann Rep Inst Fiber Sci., Osaka Univ. **1957**, 10, 1.
[15] I. Sakurada, K. Nukushina, Y. Sone, Kobunshi Kagaku **1955**, 12, 506.
[16] R.J. Roe, W.R. Krigbaum, J. Chem. Phys. **1964**, 40, 2608.
[17] R.S. Stein, F.H. Norris, I. Polym. Sci. **1956**, 21, 381.
[18] C. Clement, P.C.R. Botherel Acad Sci. (Paris) **1964**, 258, 4757.
[19] F.J. Kolpak, J. Blackwell Macromolecules **1976**, 9, 273.
[20] For example, J.S. Koeller, Phys. Rev. **1941**, 60, 397.
[21] Pizzoli M, Ceccorulli G, Scandola M. Carbohydr Res **1991**, 222, 205–213.

